Mediator-assisted water oxidation by the ruthenium "blue dimer" *cis,cis*-$[(bpy)_2(H_2O)RuORu(OH_2)(bpy)_2]^{4+}$

Javier J. Concepcion, Jonah W. Jurss, Joseph L. Templeton, and Thomas J. Meyer[1]

Department of Chemistry, University of North Carolina, Chapel Hill, NC 27599-3290

Contributed by Thomas J. Meyer, August 18, 2008 (sent for review May 26, 2008)

Light-driven water oxidation occurs in oxygenic photosynthesis in photosystem II and provides redox equivalents directed to photosystem I, in which carbon dioxide is reduced. Water oxidation is also essential in artificial photosynthesis and solar fuel-forming reactions, such as water splitting into hydrogen and oxygen ($2\ H_2O + 4\ h\nu \rightarrow O_2 + 2\ H_2$) or water reduction of CO_2 to methanol ($2\ H_2O + CO_2 + 6\ h\nu \rightarrow CH_3OH + 3/2\ O_2$), or hydrocarbons, which could provide clean, renewable energy. The "blue ruthenium dimer," *cis,cis*-$[(bpy)_2(H_2O)Ru^{III}ORu^{III}(OH_2)(bpy)_2]^{4+}$, was the first well characterized molecule to catalyze water oxidation. On the basis of recent insight into the mechanism, we have devised a strategy for enhancing catalytic rates by using kinetically facile electron-transfer mediators. Rate enhancements by factors of up to ≈30 have been obtained, and preliminary electrochemical experiments have demonstrated that mediator-assisted electrocatalytic water oxidation is also attainable.

catalysis | redox mediator | electron transfer

Water oxidation is a key reaction in photosynthesis, the basis for most of life as we know it (1–8). It is also a central reaction in artificial photosynthesis, an example being solar-driven splitting of water into hydrogen and oxygen, $2\ H_2O \rightarrow O_2 + 2\ H_2$ (9–11). In natural photosynthesis, water oxidation occurs at photosystem II (PSII) through the Kok cycle after absorption of four photons. Detailed insight into how this reaction occurs is emerging on the basis of theoretical and spectroscopic studies and recent x-ray diffraction and extended x-ray absorption fine structure results to 3.0-Å resolution (12–14).

Given the demands of the half reaction, $2\ H_2O \rightarrow O_2 + 4\ H^+ + 4e^-$, with requirements for both $4e^-/4H^+$ loss and O—O bond formation, water oxidation is difficult to achieve at a single catalyst site or cluster. In addition to PSII, water oxidation is also catalyzed by the ruthenium "blue dimer" *cis,cis*-$[(bpy)_2(H_2O)Ru^{III}ORu^{III}(OH_2)(bpy)_2]^{4+}$ (bpy is 2,2′-bipyridine) and structurally related derivatives (15–21) (Fig. 1). Other catalysts based on iridium and ruthenium complexes and in ruthenium-containing polyoxometalates have been reported recently (22–25).

The low oxidation state Ru^{III}-O-Ru^{III} form of the ruthenium blue dimer undergoes oxidative activation by proton-coupled electron transfer (PCET) in which stepwise loss of electrons and protons occurs. PCET is essential, because it allows for the buildup of multiple oxidative equivalents at a single site or cluster without building up positive charge (21, 26). As shown by the results of pH-dependent electrochemical studies (16), loss of $4e^-/4H^+$ occurs to give a reactive, transient intermediate followed by O_2 evolution.

In the absence of a serendipitous discovery, mechanistic knowledge is required for the design of robust, long-lived catalysts for water oxidation. Such knowledge is also important for the microscopic reverse reaction, oxygen reduction to water, which occurs at the cathode (reducing electrode) in fuel-cell applications (27, 28).

Mechanistic investigations of ruthenium blue dimer water oxidation with Ce(IV) as the net oxidant,

$$4\ Ce(IV) + 2\ H_2O \xrightarrow{(bpy)_2(H_2O)RuORu(H_2O)(bpy)_2^{4+}} O_2 + 4\ H^+,$$

have resulted in seemingly contradictory observations and/or different interpretations of data in different laboratories (17–21). A theoretical analysis of the mechanism based on a density functional theory (DFT) calculation has also appeared (29).

Results and Discussion

We recently were able to reconcile the seemingly disparate experimental observations on water oxidation by the ruthenium blue dimer by a comprehensive series of chemical mixing experiments with spectral and electrochemical monitoring. These observations revealed a complex mechanism involving a series of pH-dependent intermediates (21). With this insight in hand, we now report a strategy for enhancing catalytic rates based on added redox mediators that increases catalysis rates of water oxidation by the blue dimer by enhancing the slow step in the overall catalytic cycle.

A powerful method for studying the blue-dimer oxidation mechanism is spectrophotometric monitoring of changes in the solution absorbance after addition of the powerful chemical oxidant Ce(IV) with $E^{o\prime}[Ce(IV/III)] = 1.74V$ vs. the normal hydrogen electrode (NHE) in 1.0 M $HClO_4$. The dimer and its various oxidation states all absorb light strongly in the visible because of a combination of Ru–O–Ru bridge-based and charge-transfer absorptions (21). The use of Ce(IV) is restricted to strongly acidic solutions to avoid the complex hydrolysis phenomena that occur above pH = 1 (30).

Addition of 1 eq of Ce(IV) to solutions containing $((bpy)_2(H_2O)Ru^{III}ORu^{III}(OH_2)(bpy)_2)^{4+}$ (**$(H_2O)Ru^{III}ORu^{III}(OH_2)^{4+}$**) in 0.1 M HNO_3 gives $[(bpy)_2(HO)Ru^{IV}ORu^{III}(OH_2)(bpy)_2]^{4+}$ (**$(HO)Ru^{IV}ORu^{III}(OH_2)^{4+}$**) (Eq. **1**), with λ_{max} = 495 and 1,173 nm. Addition of another 2 eq of Ce(IV) (Eq. **2**) gives previously characterized $[(bpy)_2(O)Ru^{V}ORu^{IV}(O)(bpy)_2]^{3+}$ (**$(O)Ru^{V}ORu^{IV}(O)^{3+}$**), with λ_{max} = 488 and 710 nm. This reaction occurs in two steps with k(298 K, 0.1 M HNO_3) = $4.5 \times 10^3\ M^{-1}s^{-1}$ for the first step giving the intermediate Ru^{IV}–O–Ru^{IV}. It is unstable with respect to disproportionation and undergoes further, rapid oxidation to give $(O)Ru^{V}ORu^{IV}(O)^{3+}$ (21). The designation of localized oxidation states in this and related mixed-valence intermediates is a convenience. There is evidence for strong electronic coupling across the μ-oxo bridge, and oxidation states may be delocalized, $(O)Ru^{4.5}Ru^{4.5}(O)^{3+}$ (31, 32).

$$(H_2O)Ru^{III}ORu^{III}(OH_2)^{4+} + Ce^{4+} \rightarrow (HO)Ru^{IV}ORu^{III}(OH_2)^{4+} + Ce^{3+} + H^+ \quad [1]$$

Author contributions: J.J.C. and T.J.M. designed research; J.J.C. and J.W.J. performed research; J.J.C., J.W.J., J.L.T., and T.J.M. analyzed data; and J.J.C. and T.J.M. wrote the paper.

The authors declare no conflict of interest.

[1]To whom correspondence should be addressed at: University of North Carolina, Department of Chemistry, Kenan Labs A506, Chapel Hill, NC 27599-3290. E-mail: tjmeyer@email.unc.edu.

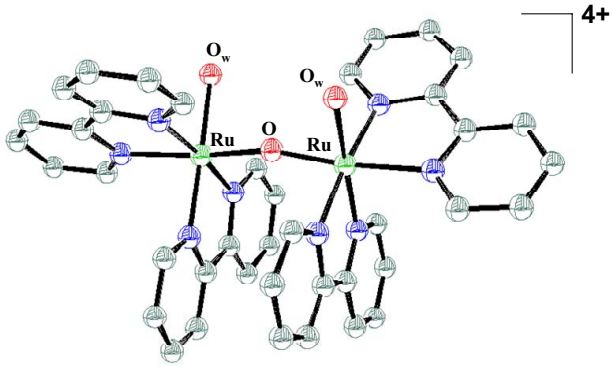

Fig. 1. Structure of the ruthenium blue dimer cation, *cis,cis*-$[(bpy)_2(H_2O)Ru^{III}ORu^{III}(OH_2)(bpy)_2]^{4+}$, in the salt $[(bpy)_2(H_2O)Ru^{III}ORu^{III}(OH_2)(bpy)_2](ClO_4)_4{\cdot}2H_2O$. The .cif file was taken from the Cambridge Crystallographic Data Centre (www.ccdc.cam.ac.uk) and corresponds to the structure published in ref. 16. [Reproduced with permission from ref. 16 (Copyright 1985, American Chemical Society).]

$$(HO)Ru^{IV}ORu^{III}(OH_2)^{4+} + 2\ Ce^{4+} \rightarrow (O)Ru^{V}ORu^{IV}(O)^{3+} + 2\ Ce^{3+} + 3\ H^{+} \quad [2]$$

Oxidation past $(O)Ru^{V}ORu^{IV}(O)^{3+}$ by 1 eq of added Ce(IV) gives an intermediate (**I**) with λ_{max} = 482 and 850 nm. The same intermediate appears after addition of 3 eq of Ce(IV) to $(HO)Ru^{IV}ORu^{III}(OH_2)^{4+}$. Redox titrations with addition of Fe^{2+} as a reducing agent show that addition of 4 eq of Fe^{2+} results in quantitative reduction of **I** to $(H_2O)Ru^{III}ORu^{III}(OH_2)^{4+}$. Increasing the acid concentration to 1.0 M HNO_3 results in absorption spectral shifts to λ_{max} = 451 and 750 nm. The absorption changes with acid concentration are reversible and consistent with the acid–base equilibrium between **I** and a second, protonated form (**II**) shown in Eq. **5** with $0 < pK_a < 1$.

$$[(bpy)_2(O)Ru^{V}ORu^{IV}(O)(bpy)_2]^{3+} + Ce(IV) \rightarrow \{(bpy)_2(O)Ru^{V}ORu^{V}(O)(bpy)_2^{4+}\} + Ce(III) \quad [3]$$

$$\{(bpy)_2(O)Ru^{V}ORu^{V}(O)(bpy)_2^{4+}\} + H_2O \rightarrow [(bpy)_2(HO_2)Ru^{III}ORu^{V}(O)(bpy)_2]^{3+} + H^{+} \quad [4]$$

$$[(bpy)_2(HO_2)Ru^{IV}ORu^{IV}(OH)(bpy)_2]^{4+}(\mathbf{II}, \lambda_{max} = 451,750\ nm) \rightleftharpoons [(bpy)_2(HO_2)Ru^{III}ORu^{V}(O)(bpy)_2]^{3+} + H^{+}(\mathbf{I}, \lambda_{max} = 482, 850\ nm) \quad [5]$$

Appearance of the intermediate at λ_{max} = 482 and 850 nm occurs rapidly after one-electron oxidation of $(O)Ru^{V}ORu^{IV}(O)^{3+}$ to $(O)Ru^{V}ORu^{V}(O)^{4+}$. The latter does not build up as an observable transient but has been trapped as an unstable black ClO_4^- salt in ice-cold 1.0 M $HClO_4$ (17).

In Eq. **5** the intermediate is formulated as a terminal peroxide, $(HO_2)Ru^{III}ORu^{V}(O)^{3+}$. This formulation is consistent with the results of the redox titration and the acid–base equilibrium in Eq. **5**. It is also consistent with the results of DFT calculations by Yang and Baik (29), which predict a peroxidic intermediate. The oxidation state distribution in deprotonated form **I** is unknown but consistent with proton loss and stabilization by oxo formation in $Ru^{V} = O$ (33).

After addition of 30 eq of Ce(IV), the peroxidic intermediate is the dominant form in the catalytic steady state as shown by visible absorption measurements. Under these conditions, loss of Ce(IV), monitored at 360 nm, is first order in intermediate and first order in Ce(IV) with k(298 K, 0.1 M HNO_3) = 183 $M^{-1}{\cdot}s^{-1}$. These observations point to rate-limiting oxidation of $(HO_2)Ru^{III}ORu^{V}(O)^{3+}$ followed by rapid O_2 evolution (Eqs. **6** and **7**) as the final steps in the oxidation cycle. At the end of the cycle with Ce(IV) largely depleted, the rate-limiting step changes to Ce(IV) oxidation of $(O)Ru^{V}ORu^{IV}(O)^{3+}$ as shown by its buildup in solution at λ_{max} = 488 and 710 nm.

$$(HO_2)Ru^{III}ORu^{V}(O)^{3+} + Ce^{4+} \rightarrow \{(HO_2)Ru^{IV}ORu^{V}(O)^{4+}\} + Ce^{3+} \quad [6]$$

$$\{(HO_2)Ru^{IV}ORu^{V}(O)^{4+}\} + H_2O \xrightarrow{\text{rapid}} (HO)Ru^{IV}ORu^{III}(OH_2)^{4+} + O_2 \quad [7]$$

On the basis of this mechanistic insight, we have devised a strategy for enhancing catalytic water oxidation by addition of the kinetically facile electron-transfer mediators, $Ru(bpy)_2(L\text{-}L)^{2+}$ [L-L is bpy, 2,2′-bipyrimidine (bpm), and 2,2′-bipyrazine (bpz)] and $[Ru(bpm)_3]^{2+}$. With these ligand variations, reduction potentials for the corresponding Ru(III/II) couples ($E°'$ vs. NHE) are varied systematically: 1.27, 1.40, 1.49, and 1.69 V, respectively. Oxidation to their Ru(III) forms by Ce(IV) is spontaneous or nearly spontaneous with $E°'$(Ce(IV/III) = 1.60 V in 1 M HNO_3. These couples undergo facile electron transfer with self-exchange rate constants between the $Ru(bpy)_2(L)^{3+}$ and $Ru(bpy)_2(L)^{2+}$ forms on the order of 10^8 to 10^9 s^{-1}, whereas the self-exchange rate constant for the Ce(IV/III) couple is slower by orders of magnitude (34).

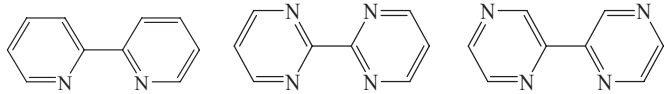

bpy bpm bpz

Results obtained by monitoring Ce(IV) loss spectrophotometrically at 360 nm under catalytic conditions with 30 eq of added Ce(IV) and added mediator are summarized in Table 1. Under these conditions the peroxidic intermediate, as **I** or **II** depending on acidity, still dominates at the catalytic steady state (Figs. 2 and 3). The data in Table 1 demonstrate rate enhancements for water oxidation by factors of up to ≈30 as a result of mediated oxidation of the peroxidic intermediate (Eqs. **8** and **9**). The rate enhancements are attributable to an interplay between rate-limiting oxidation of RuL_3^{2+} (Eq. **8**) and rate-limiting oxidation of the peroxidic intermediate (Eq. **9**). For example, the rate constant for oxidation of $[Ru(phen)_3]^{2+}$ by Ce(IV) in 0.1 M HNO_3 (≈10^5 $M^{-1}{\cdot}s^{-1}$; see ref. 35) is ≈500 times more rapid than oxidation of $(HO_2)Ru^{III}ORu^{V}(O)^{3+}$ by $[Ru(bpy)_3]^{3+}$ (≈1.9 × 10^3 $M^{-1}{\cdot}s^{-1}$). On the other hand, there is no catalysis by $[Ru(bpy)_2(bpz)]^{2+}$ in 0.1 M HNO_3 (Table 1) because of slow oxidation of RuL_3^{2+} by Ce(IV).

$$RuL_3^{2+} + Ce^{4+} \rightarrow RuL_3^{3+} + Ce^{3+} \quad [8]$$

Table 1. Observed rate constants for Ce(IV) loss by oxidation of peroxido intermediates I (0.1 M HNO_3) or II (1.0 M HNO_3) at 298 K

Redox mediator	$E_{1/2}$,V vs NHE	k (1.0 M HNO_3), $M^{-1}\cdot s^{-1}$	k (0.1 M HNO_3), $M^{-1}\cdot s^{-1}$
None		80	180
$[Ru(bpy)_3]^{2+}$	1.27	*	1,900
$[Ru(bpy)_2(bpm)]^{2+}$	1.40	1,000	5,500
$[Ru(bpy)_2(bpz)]^{2+}$	1.49	1,800	†
$[Ru(bpm)_3]^{2+}$	1.69	900	†

As monitored by Ce(IV) loss at 360 nm (see *Materials and Methods*). Conditions: $[(H_2O)Ru^{III}ORu^{III}(OH_2)^{4+}] = 1.25 \times 10^{-5}$ M, [redox mediator] = 1.25×10^{-5} M, and 30 eq of Ce(IV).

*No catalysis because oxidation of the protonated form of the peroxidic intermediate $[(HO_2)Ru^{IV}ORu^{IV}(OH)]^{4+}$ at pH = 0 by $Ru(bpy)_3^{3+}$ is thermodynamically unfavorable and slow.

†No catalysis because oxidation of $[Ru(bpy)_2(bpz)]^{2+}$ or $[Ru(bpm)_3]^{2+}$ by Ce(IV) at pH = 1 is slow. $E°$[Ce(IV/III)] = 1.6 V in 1 M HNO_3, but this couple is highly medium-dependent (30).

$$(HO_2)Ru^{III}ORu^{V}(O)^{3+} + RuL_3^{3+} \rightarrow \{(HO_2)Ru^{IV}ORu^{V}(O)^{4+}\} + RuL_3^{2+} \quad [9]$$

With added mediator, oxygen evolution occurs quantitatively as shown by oxygen electrode measurements. Addition of 30 eq of Ce(IV) resulted in appearance of the expected ≈7.5 eq of O_2 consistent with the expected stoichiometry in Eq. **10** and the catalytic cycle in Scheme 1.

$$4\ Ce(IV) + 2\ H_2O \rightarrow 4\ Ce(III) + O_2 + 4\ H^+ \quad [10]$$

These results are important in further demonstrating and then exploiting the complex mechanistic details of water oxidation by the ruthenium blue dimer. They also add to the limited insight available for water oxidation and make a possible connection with water oxidation in PSII, in which a peroxido intermediate has also been proposed (6, 7). Preliminary electrochemical experiments in 0.1 M HNO_3 with a glassy carbon working electrode demonstrate that mediator-assisted electrocatalytic water oxidation (Scheme 2) is attainable with a turnover number of 19, which has already been achieved.

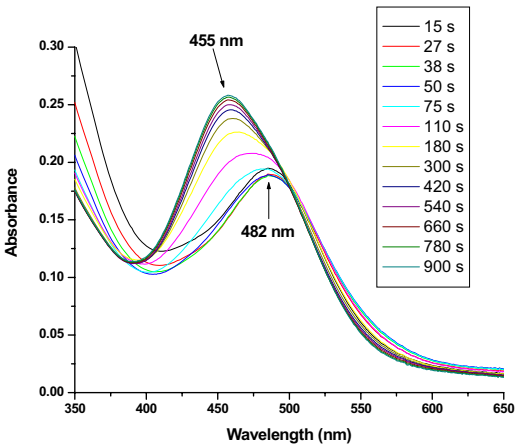

Fig. 2. Spectral changes after the addition of 30 eq of Ce(IV) to a solution containing 1.25×10^{-5} M $(H_2O)Ru^{III}ORu^{III}(OH_2)^{4+}$ and 1.25×10^{-5} M $[Ru(bpy)_2(bpm)]^{2+}$ as redox mediator in 0.1 M HNO_3. Initially, the peroxidic intermediate $(HO_2)Ru^{III}ORu^{V}(O)^{3+}$ (λ_{max} = 482 nm) is the dominant species in solution, because its oxidation by the redox mediator is the rate-limiting step. Once all of the Ce(IV) has been consumed (≈50 s), the anated species $(O_2NO)Ru^{IV}ORu^{IV}(OH)^{4+}$ (λ_{max} = 455 nm) begins to form, and it is the dominant form of the dimer at the end of the experiment (≈900 s).

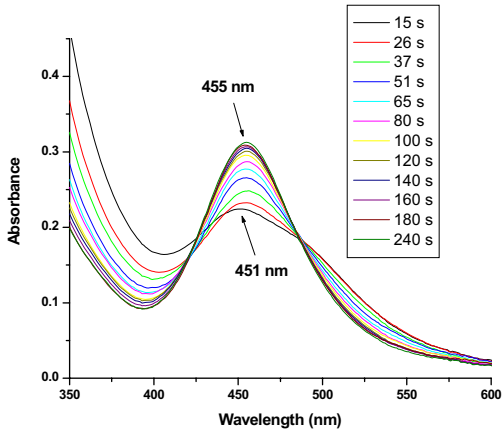

Fig. 3. Spectral changes after the addition of 30 eq of Ce(IV) to a solution containing 1.25×10^{-5} M $(H_2O)Ru^{III}ORu^{III}(OH_2)^{4+}$ and 1.25×10^{-5} M $[Ru(bpy)_2(bpz)]^{2+}$ as redox mediator in 1.0 M HNO_3. Initially, the peroxidic intermediate $(HO_2)Ru^{IV}ORu^{IV}(OH)^{4+}$ (λ_{max} = 451 nm) is the dominant species in solution, because its oxidation by the redox mediator is the rate-limiting step. As a result of a higher anion concentration in this case (1.0 M NO_3^-), the anated species $(O_2NO)Ru^{IV}ORu^{IV}(OH)^{4+}$ (λ_{max} = 455 nm) begins to form before all of the Ce(IV) has been consumed (≈180 s), and it is the dominant form of the dimer at the end of the experiment (≈300 s).

In the reaction center of PSII, light is harvested by an antenna array consisting of chlorophylls and organic pigments, which sensitize the lowest singlet excited state of chlorophyll P_{680} or a neighboring pheophytin$_{D1}$ (36). This excited state subsequently undergoes oxidative quenching, giving P_{680}^+ by electron transfer to quinone Q_A. In the next step, P_{680}^+ oxidizes redox mediator tyrosine Tyr_Z (Y_Z), which in turn activates the oxygen-evolving complex (OEC) by coupled electron–proton transfer (6, 26).

Cape and Hurst (37) have shown that $[Ru(bpy)_3]^{3+}$ generated by persulfate oxidation of $[Ru(bpy)_3]^{2+*}$ can oxidize the blue dimer, which in turn oxidizes water. We believe that it should be possible to mimic the features of the reaction center of PSII in designed molecular assemblies on the surfaces of appropriately chosen semiconductor metal oxide electrodes with the ruthenium blue dimer or a derivative acting as an OEC analog (21, 38).

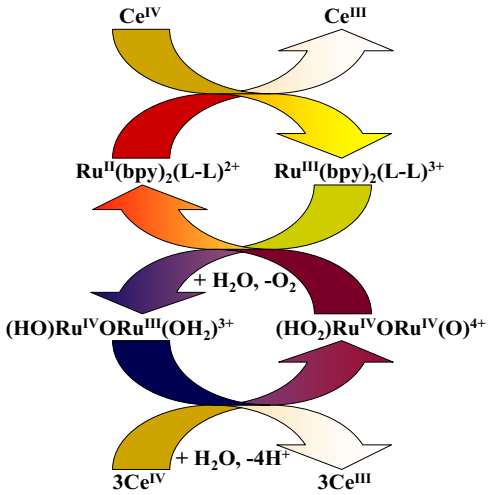

Scheme 1. Catalytic cycle for mediator-assisted water oxidation by the blue dimer.

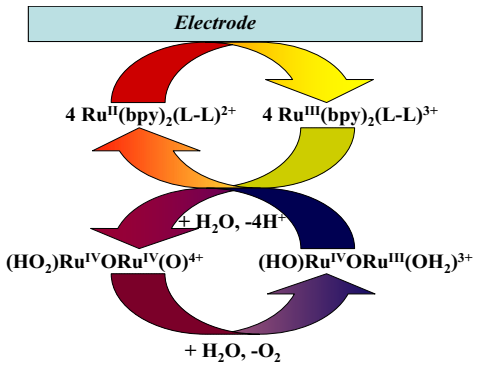

Scheme 2. Electrocatalytic cycle for mediator-assisted water oxidation by the blue dimer.

Materials and Methods

Distilled water was further purified by using a Milli-Q ultrapure water-purification system. Stock solutions of Ce(IV) for kinetic and stoichiometric measurements were prepared from $(NH_4)_2Ce(NO_3)_6$ (99.99+%, Aldrich). Nitric acid (trace-metal grade, 70%) was purchased from Fisher Scientific. *cis*-$[Ru(bpy)_2Cl_2]$ and *cis,cis*-$[(bpy)_2(H_2O)Ru^{III}ORu^{III}(OH_2)bpy)_2](ClO_4)_2$ were prepared as described previously (39, 40). 2,2′-Bipyrimidine (97%) and $RuCl_3{\cdot}H_2O$ were purchased from Aldrich and used as received. 2,2′-Bipyrazine (41) and $[Ru(bpy)_3](Cl)_2{\cdot}6H_2O$ (42) were prepared as described in the literature. $[Ru(bpm)_3](PF_6)_2$ (43), $[Ru(bpy)_2(bpz)](PF_6)_2$ (43), and $[Ru(bpy)_2(bpm)](PF_6)_2$ (44) were prepared as reported in the literature and converted to the water-soluble chloride or nitrate salts by metathesis in acetone or acetonitrile with tetrabutylammonium chloride or nitrate. All other reagents were American Chemical Society grade and used without additional purification.

UV-visible spectra vs. time were recorded on an Agilent Technologies model 8453 diode-array spectrophotometer. Data were processed by use of the program SPECFIT/32 Global Analysis System (SPECTRUM Software Associates). Kinetic measurements were also performed on a Shimadzu UV-visible near-infrared spectrophotometer model UV-3600 by monitoring the disappearance of Ce(IV) at 360 nm. Electrochemical measurements were performed on an EG&G Princeton Applied Research model 273A potentiostat/galvanostat. Voltammetric measurements were made with a planar EG&G PARC G0229 glassy carbon millielectrode, a platinum wire EG&G PARC K0266 counter electrode, and Ag/AgCl EG&G PARC K0265 reference electrode. Oxygen measurements were performed with a calibrated O_2 electrode (Microelectrodes, MI-730). In a typical experiment, 30 eq of Ce(IV) wasd added to stirred solutions containing 3×10^{-4} M $Ru^{III}ORu^{III}$ blue dimer in 0.1 M HNO_3 with 6×10^{-4} M redox mediator. The air-tight reaction cell was purged with argon before the addition of the Ce(IV) until the digital readout had stabilized. O_2 evolution vs. time was recorded, and the theoretical maximum was achieved within 2% for multiple runs with and without redox mediator.

ACKNOWLEDGMENTS. The Chemical Sciences, Geosciences, and Biosciences Division of the Office of Basic Energy Sciences, US Department of Energy, supported this research.

1. Tommos C, Babcock GT (1998) Oxygen production in nature: A light-driven metalloradical enzyme process. *Acc Chem Res* 31:18–25.
2. Nelson N, Yocum CF (2006) Structure and function of photosystems I and II. *Annu Rev Plant Biol* 57:521–565.
3. Kern J, Biesiadka J, Loll B, Saenger W, Zouni A (2007) Structure of the Mn_4-Ca cluster as derived from x-ray diffraction. *Photosynth Res* 92:389–405.
4. Barber J (2006) Photosystem II: An enzyme of global significance. *Biochem Soc Trans* 34:619–631.
5. McEvoy JP, Brudvig GW (2006) Water-splitting chemistry of photosystem II. *Chem Rev* 106:4455–4483.
6. Meyer TJ, Huynh MHV, Thorp HH (2007) The possible role of proton-couple electron transfer (PCET) in water oxidation by photosystem II. *Angew Chem Int Ed* 46:5284–5304.
7. Renger G (2007) Oxidative photosynthetic water splitting: Energetics, kinetics and mechanism. *Photosynth Res* 92:407–425.
8. Cady CW, Crabtree RH, Brudvig GW (2008) Functional models for the oxygen-evolving complex of photosystem II. *Coord Chem Rev* 252:444–455.
9. Alstrum-Acevedo JH, Brennaman MK, Meyer TJ (2005) Chemical approaches to artificial photosynthesis 2. *Inorg Chem* 44:6802–6827.
10. Gust D, Moore TA, Moore AL (2001) Mimicking photosynthetic solar energy transduction. *Acc Chem Res* 34:40–48.
11. Wasielewski MR (1992) Photoinduced electron transfer in supramolecular systems for artificial photosynthesis. *Chem Rev* 92:435–461.
12. Ferreira KN, Iverson TM, Maghlaoui K, Barber J, Iwata S (2004) Architecture of the photosynthetic oxygen-evolving center. *Science* 303:1831–1838.
13. Loll B, Kern J, Saenger W, Zouni A, Biesiadka J (2005) Towards complete cofactor arrangement in the 3.0 Å resolution structure of photosystem II. *Nature* 438:1040–1044.
14. Yano J, *et al*. (2005) High-resolution Mn EXAFS of the oxygen-evolving complex in photosystem II: Structural implications for the Mn_4Ca cluster. *J Am Chem Soc* 127:14974–14975.
15. Gersten SW, Samuels GJ, Meyer TJ (1982) Catalytic oxidation of water by an oxo-bridge ruthenium dimer. *J Am Chem Soc* 104:4029–4030.
16. Gilbert JA, *et al*. (1985) Structure and redox properties of the water-oxidation catalyst $[(bpy)_2(OH_2)RuORu(OH_2)(bpy)_2]^{4+}$. *J Am Chem Soc* 107:3855–3864.
17. Binstead RA, Chronister CW, Ni J, Hartshorn CM, Meyer TJ (2000) Mechanism of water oxidation by the μ-oxo dimer $[(bpy)_2(OH_2)RuORu(OH_2)(bpy)_2]^{4+}$. *J Am Chem Soc* 122:8464–8473.
18. Yamada H, Siems WF, Koike T, Hurst JK (2004) Mechanisms of water oxidation catalyzed by the *cis,cis*-$[(bpy)_2Ru(OH_2)]_2O^{4+}$ ion. *J Am Chem Soc* 126:9786–9795.
19. Hurst JK (2005) Water oxidation catalyzed by dimeric μ-oxo bridge ruthenium diimine complexes. *Coord Chem Rev* 249:313–328.
20. Hurst JK, Cape JL, Clark AE, Das S, Qin C (2008) Mechanisms of water oxidation catalyzed by ruthenium diimine complexes. *Inorg Chem* 47:1753–1764.
21. Liu F, *et al*. (2008) Mechanisms of water oxidation from the blue dimer to photosystem II. *Inorg Chem* 47:1727–1752.
22. McDaniel ND, Coughlin FJ, Tinker LL, Bernhard S (2008) Cyclometalated iridium(III) aquo complexes: Efficient and tunable catalysts for the homogeneous oxidation of water. *J Am Chem Soc* 130:210–217.
23. Zong R, Thummel RP (2005) A new family of Ru complexes for water oxidation. *J Am Chem Soc* 127:12802–12803.
24. Geletii YV, *et al*. (2008) An all-inorganic, stable, and highly active tetraruthenium homogeneous catalyst for water oxidation. *Angew Chem Int Ed* 47:3896–3899.
25. Sartorel A, *et al*. (2008) Polyoxometalate embedding of a tetraruthenium(IV)-oxo-core by template-directed metalation of $[\gamma\text{-}SiW_{10}O_{36}]^{8-}$: A totally inorganic oxygen-evolving catalyst. *J Am Chem Soc* 130:5006–5007.
26. Huynh MHV, Meyer TJ (2007) Proton-coupled electron transfer. *Chem Rev* 107:5004–5064.
27. Collman JP, *et al*. (2007) A cytochrome *c* oxidase model catalyzes oxygen to water reduction under rate-limiting electron flux. *Science* 315:1565–1568.
28. Chang CJ, Loh ZH, Shi C, Anson FC, Nocera DG (2004) Targeted proton delivery in the catalyzed reduction of oxygen to water by bimetallic pacman porphyrins. *J Am Chem Soc* 126:10013–10020.
29. Yang X, Baik MH (2006) *cis,cis*-$[(bpy)_2Ru^{V}O]_2O^{4+}$ catalyzes water oxidation formally via in situ generation of radicaloid Ru^{IV}-O·. *J Am Chem Soc* 128:7476–7485.
30. Bondareva TN, Stromberg AG (1955) The potentiometric study of the precipitation of Ce(IV) and Ce(III) with respect to the effect of pH of the solution on the oxidation-reduction potential of the system Ce^{4+}/Ce^{3+}. *Zh Obshch Khim* 25:666–671.
31. Bartolotti LJ, Pedersen LG, Meyer TJ (2001) Quantum mechanical study of the oxidation pathway of the oxygen-evolving catalyst, $[(bpy)_2(H_2O)Ru^{III}\text{-}O\text{-}Ru^{III}(H_2O)(bpy)_2]^{+4*}$. *Int J Quantum Chem* 83:143–149.
32. Concepcion JJ, Dattelbaum DM, Rocha RC, Meyer TJ (2008) Probing the localized-to-delocalized transition. *Philos Trans R Soc London Ser A* 336:163–175.
33. Meyer TJ, Huynh MHV (2003) The remarkable reactivity of high oxidation state ruthenium and osmium polypyridyl complexes. *Inorg Chem* 42:8140–8160.
34. Sigler PB, Masters BJ (1957) The hydrogen peroxide-induced Ce*(III)-Ce(IV) exchange system. *J Am Chem Soc* 79:6353–6357.
35. Miller JD, Prince RH (1966) The oxidation of some ruthenium(II) complexes by ceric ion. *J Chem Soc A* 10:1370–1372
36. Holzwarth AR, *et al*. (2006) Kinetics and mechanism of electron transfer in intact photosystem II and in the isolated reaction center: Pheophytin is the primary electron acceptor. *Proc Natl Acad Sci USA* 103:6895–6900.
37. Cape JL, Hurst JK (2008) Detection and mechanistic relevance of transient ligand radicals formed during $[Ru(bpy)_2(OH_2))]_2O^{4+}$-catalyzed water oxidation. *J Am Chem Soc* 130:827–829.
38. Treadway JA, Moss JA, Meyer TJ (1999) Visible region photooxidation on TiO_2 with a chromophore-catalyst molecular assembly. *Inorg Chem* 38:4386–4387.
39. Sullivan BP, Salmon DJ, Meyer TJ (1978) Mixed phosphine 2,2′-bipyridine complexes of ruthenium. *Inorg Chem* 17:3334–3341.
40. Gilbert JA, *et al*. (1985) Structure and redox properties of the water-oxidation catalyst $[(bpy)_2(OH_2)RuORu(OH_2)(bpy)_2]^{4+}$. *J Am Chem Soc* 107:3855–3864.
41. Boully L, Darabantu M, Turck A, Ple N (2005) Aryl-aryl bonds formation in pyridine and diazine series: Diazines. Part 41. *J Heterocycl Chem* 42:1423–1428.
42. Broomhead JA, Young CG (1982) Tris(2,2′-bipyridine)ruthenium(II) dichloride hexahydrate. *Inorg Synth* 21:127–128.
43. Rillema DP, Allen G, Meyer TJ, Conrad D (1983) Redox properties of ruthenium(II) tris chelate complexes containing the ligands 2,2′-bipyrazine, 2,2′-bipyridine, and 2,2′-bipyrimidine. *Inorg Chem* 22:1617–1622.
44. Ji Z, Huang SD, Guadalupe AR (2000) Synthesis, x-ray structures, spectroscopic and electrochemical properties of ruthenium(II) complexes containing 2,2′-bipyrimidine. *Inorg Chim Acta* 305:127–134.